14th European Signal Processing Conference (EUSIPCO 2006), Florence, Italy, September 4-8, 2006, copyright by EURASIP

IMAGE SHARPENING BY COUPLED NONLINEAR-DIFFUSION ON THE CHROMATICITY-BRIGHTNESS COLOR REPRESENTATION

Takahiro Saito, Reina Nosaka, and Takashi Komatsu

Dept. of Electronics and Informatics Frontiers, High-Tech Research Center, Kanagawa University
3-27-1 Rokkakubashi, 221-8686, Yokohama, Japan
phone: +(81) 45 481 5661, fax: +(81) 45 491 7915, email: {saitot01, R200570093, komatt01}@kanagawa-u.ac.jp
web: www.ku-hrc.jp

ABSTRACT

Previously we presented a selective image sharpening method with a coupled nonlinear diffusion process, and it sharpens only blurred edges without enhancing noise. Our prototypal color-image sharpening methods were formulated on the linear color models, namely, the channel-by-channel model and the 3D vector model. Our prototypal methods sharpen blurred color edges, but they do not necessarily enhance contrasts of signal variations in complex texture regions so well as in simple step-edge regions. To remedy the drawback, we extend our coupled nonlinear-diffusion sharpening method to the nonlinear non-flat color model, namely, the chromaticity-brightness model, which is known to be closely relating to human color perception. We modify our time-evolution PDE's for the non-flat space of the chromaticity vector, and present its digital implementations.

1. INTRODUCTION

For image sharpening, various filtering methods such as the peaking technique were developed [1]. However, the filtering methods have the common disadvantage that they cannot work well for noisy blurred images; they will enhance noise. Selectivity in image sharpening is the key to its success.

For the selective image sharpening, recently the new line appeared; the nonlinear PDE (Partial Differential Equation) methods were developed [2]~[12]. Among them, the most basic one is the bounded-variation image restoration method [3]. This method restores degraded images by minimizing the energy functional composed of the restoration energy term and the smoothness energy term. The time-evolution equation for the minimization is given by the Euler-Lagrange PDE, and its steady-state solution is used as a sharpened image. The method needs the accurate knowledge of the model of image blurs. If we define the restoration energy properly, the method will be able to achieve the selective image sharpening. However, if the blur model is not accurate, it will often produce visible artifacts.

The other category of the PDE methods is a collection of the methods that do not need any accurate knowledge of the blur model and that use the transient solution of the time-evolution PDE as a sharpened image. The typical methods of this category are the forward-and-backward diffusion method proposed by Gilboa and others [7], and our coupled nonlinear-diffusion method [8]~[11]. We applied our method to the selective sharpening of monochrome and color images [8]~[11]. By quantitative experiments we showed that our method has a desirable capability to sharpen blurred edges without enhancing noise. Our method is a flexible selective sharpening method that can be applied to various image-processing tasks by introducing a certain adaptive control into it.

Our prototypal color-image sharpening methods with the coupled nonlinear-diffusion process were formulated on the linear color models, namely, the channel-by-channel model and the 3D vector model. Our prototypal methods sharpen blurred color edges, but they do not necessarily enhance contrasts of signal variations in complex texture regions so well as in simple step-edge regions. To remedy the drawback, in this paper we extend our coupled nonlinear-diffusion sharpening method to the nonlinear non-flat color model, namely, the chromaticity-brightness model, which is known to be closely relating to human color perception [13]~[17]. We modify our time-evolution PDE's for the non-flat space of the chromaticity vector and present its digital implementations. Through experimental simulations, we compare our new sharpening method based on the chromaticity-brightness model with our prototypal sharpening methods based on the linear color models.

2. SCALAR IMAGE SHARPENING BY COUPLED NONLINEAR-DIFFUSION

The forward diffusion process is formulated by the time-evolution PDE with a positive diffusion coefficient,

$$\partial_\tau f = div\left(a \cdot \nabla f\right) = a \cdot \Delta f \quad , \quad a > 0 \,, \tag{1}$$

and it smooths out noisy variations and it blurs edges, whereas the backward diffusion process is formulated by the time-evolution PDE with a negative diffusion coefficient,

$$\partial_\tau f = div\left(-a \cdot \nabla f\right) = -a \cdot \Delta f \quad , \quad a > 0 \,, \tag{2}$$

and it sharpens blurred edges to steeper edges. The popular peaking method formulated by

$$f - a \cdot \Delta f \quad , \quad a > 0 \tag{3}$$

has the property of the backward diffusion, and creates overshoots near edges [1]. However, the backward diffusion has crucial drawbacks: instability, oscillations and noise amplification. The promising approach to solve them is to introduce the competition between the forward diffusion and the backward diffusion into the process. We need to control the competition so that the backward diffusion will dominate over the forward diffusion only near blurred edges. The typical methods utilizing the competition are the forward-and-backward diffusion method proposed by Gilboa and others [7], and our coupled nonlinear-diffusion method [8]~[11].

Our coupled nonlinear-diffusion method introduces the competition between the Perona and Malik (P-M) nonlinear-diffusion term [4] and the peaking term into the process, and for the peaking term it uses regularized spatial derivatives given by the P-M process of image derivatives. The utilization of the regularized derivatives corresponds to the spatial regularization [12], but instead of

the Gaussian smoothing our method employs the P-M process. The time-evolution equations of our method are given by

$$\begin{aligned}
\partial_\tau f &= \partial_x\left(g\left(|\nabla f|\right)\cdot\partial_x f\right)+\partial_y\left(g\left(|\nabla f|\right)\cdot\partial_y f\right)-s\cdot\left(\partial_x u+\partial_y v\right)\\
&\quad -\lambda_f\cdot\left(f-I\right),\\
\partial_\tau u &= \partial_x\left(g\left(|\nabla u|\right)\cdot\partial_x u\right)+\partial_y\left(g\left(|\nabla u|\right)\cdot\partial_y u\right)-\lambda_u\cdot\left(u-\partial_x f\right),\\
\partial_\tau v &= \partial_x\left(g\left(|\nabla v|\right)\cdot\partial_x v\right)+\partial_y\left(g\left(|\nabla v|\right)\cdot\partial_y v\right)-\lambda_v\cdot\left(v-\partial_y f\right),\\
g(z) &= 1\Big/\left(1+\left(z/K\right)^2\right)\text{: edge-stopping function,}\\
f(x,y;\tau)&\text{: time-evolving image,}\quad I(x,y)\text{: input image,}\\
u(x,y;\tau),&\,v(x,y;\tau)\text{ : time-evolving auxiliary functions,}\\
\tau&\text{ : artificial time parameter,}
\end{aligned}\tag{4}$$

where the auxiliary functions *u*, *v* approximate the first horizontal and vertical partial derivatives of the function *f*, respectively. The initial condition is given by

$$\begin{aligned}
&f(x,y;0)=I(x,y);\\
&u(x,y;0)=\partial_x I(x,y);\; v(x,y;0)=\partial_y I(x,y).
\end{aligned}\tag{5}$$

The transient solution of the time-evolution PDE of (4) is used as a sharpened image. Previously we presented a decision scheme to halt the time-evolution at the ideal moment when it achieves the best selective image sharpening.

The first equation in (4) formulates the time-evolution of the image *f*, and is composed of the P-M nonlinear-diffusion term, the peaking term and the fidelity term. The amount of overshoots to be added is controlled by the shooting parameter *s* that is typically set to a positive value less than 1.0. The competition between the P-M term and the peaking term will result in smoothing out noisy variations within a homogeneous region, whereas the competition will produce overshoots only near blurred edges. The second and the third equations in (4) formulate the time-evolution for regularizing the two auxiliary functions *u*, *v* approximating the spatial derivatives of the image *f*, and they are composed of the P-M term and the fidelity term. The time-evolving auxiliary functions *u*, *v* are used for the computation of the peaking term in the first equation.

3. SHARPENING METHODS BASED ON THE LINEAR COLOR MODELS

In this paper we focus on the primary color space. In this color space, a color vector at each pixel is represented by a 3D vector whose components are values of the three primary colors. In the following, the time-evolving color vector **C**, the input color vector **I** and the auxiliary vectors **u**, **v** at each pixel (x,y) are represented by the two-variable vector functions as follows:

$$\mathbf{C}(x,y)=\left(C_R(x,y),C_G(x,y),C_B(x,y)\right)^T. \tag{6}$$

Our prototypal color-image sharpening methods were formulated on the linear color models, namely, the channel-by-channel color model and the 3D vector color model.

3.1 I-Scheme: Independent scheme based on the channel-by-channel color model

The I-scheme is formulated on the channel-by-channel color model, and it applies the time-evolution of (4) independently to each color component. Moreover, the I-scheme employs the simultaneous stopping scheme that halts the iterations of all the three components of the color vector **C** all at once.

3.2 V-Scheme: Vector scheme based on the 3D vector color model

The V-scheme is formulated on the 3D vector color model, and it collectively treats all the color components. It uses the magnitude of a color edge to control the nonlinear-diffusion term in the time-evolution of **C**. The color-edge magnitude is computed from the structure tensor **H**:

$$\mathbf{H}=\begin{pmatrix}E & F\\ F & G\end{pmatrix}\;;\; E=\left\|\partial_x\mathbf{C}\right\|^2,\; F=\left(\partial_x\mathbf{C},\partial_y\mathbf{C}\right),\; G=\left\|\partial_y\mathbf{C}\right\|^2. \tag{7}$$

The color edge appears along the eigenvector corresponding to the maximum eigenvalue λ_+ of **H**, and the color-edge magnitude γ is defined by using the maximum eigenvalue λ_+ and the minimum eigenvalue λ_- of **H**:

$$\gamma=\sqrt{\lambda_+-\lambda_-}=\left(\left(E-G\right)^2+4F^2\right)^{1/4}. \tag{8}$$

The V-scheme employs the nonlinear-diffusion time-evolution:

$$\begin{aligned}
\partial_\tau\mathbf{C} &= \partial_x\left(g(\gamma)\cdot\partial_x\mathbf{C}\right)+\partial_y\left(g(\gamma)\cdot\partial_y\mathbf{C}\right)-s\cdot\left(\partial_x\mathbf{u}+\partial_y\mathbf{v}\right)\\
&\quad -\lambda_C\cdot\left(\mathbf{C}-\mathbf{I}\right).\\
\gamma &= \left(\left(E-G\right)^2+4F^2\right)^{1/4};\; E=\left\|\mathbf{u}\right\|^2,\; F=\left(\mathbf{u},\mathbf{v}\right),\; G=\left\|\mathbf{v}\right\|^2
\end{aligned}\tag{9}$$

As the time-evolution for the two auxiliary vector functions **u**, **v**, the V-scheme employs the same time-evolution equations as the I-scheme. Moreover, the V-scheme employs the simultaneous stopping scheme that halts the iterations of the three components of the color vector **C** all at once.

The I-scheme and the V-scheme sharpen blurred color edges to steeper edges, and the V-scheme outperforms the I-scheme. However, both the I-scheme and the V-scheme do not necessarily enhance contrasts of signal variations in complex texture regions so well as in simple step-edge regions. To solve the problem, we extend our coupled nonlinear-diffusion sharpening method to the nonlinear non-flat color model, namely, the chromaticity-brightness model, which is known to be closer to human color perception [13], and forms a more flexible color-image sharpening method in which parameter setting is more adaptable to human perception.

4. SHARPENING METHOD BASED ON THE CHROMATICITY-BRIGHTNESS COLOR MODEL

We present a new sharpening method based on the chromaticity-brightness color model, and we call it the CB-scheme for short. The chromaticity-brightness color model decompose the 3D primary color vector **C** into two components, namely, the brightness component $r=\|\mathbf{C}\|$ and the chromaticity component $\mathbf{w}=\mathbf{C}/r$ [13]~[17]. The chromaticity component **w** lives on the unit sphere $\mathbf{S}^2$ embedded in $\mathbf{R}^3$. The brightness component *r* and the chromaticity component $\mathbf{w}=(w_1, w_2, w_3)^T$ have the properties:

$$r>0\;\;;\;\;\left\|\mathbf{w}\right\|=1\quad\text{and}\quad w_n\ge 0. \tag{10}$$

The brightness component *r* is treated as a scalar image, and hence the time-evolution equations of (4) is directly applied to it. On the other hand, the chromaticity component **w** is non-flat, because it takes a vector on the unit sphere $\mathbf{S}^2$. Thereby we cannot directly apply the time-evolution equations of (9) for the V-scheme defined in $\mathbf{R}^3$, and we need to modify them by replacing the flat derivative operators ∂_x, ∂_y in $\mathbf{R}^3$ with the covariant derivative operators $\partial_x^*, \partial_y^*$ acting on the vector field defined at the point $\mathbf{w}(x,y)$ on the unit sphere $\mathbf{S}^2$. In this case, the covariant derivative ∂_x^* is computed by projecting the flat derivative ∂_x onto the tangent space $\mathbf{T}_{\mathbf{w}(x,y)}$ of the unit sphere $\mathbf{S}^2$ at $\mathbf{w}(x,y)$ as follows [16], [17]:

$$\begin{aligned}
\partial_x^*\mathbf{f} &= \Pi_{\mathbf{w}(x,y)}\left\{\partial_x\mathbf{f}\right\}\quad,\\
\Pi_{\mathbf{w}(x,y)}\left\{\mathbf{z}\right\} &= \mathbf{z}-\left(\mathbf{z},\mathbf{w}(x,y)\right)\cdot\mathbf{w}(x,y)\\
&\quad :\text{ projection onto the tangent space }\mathbf{T}_{\mathbf{w}(x,y)}.
\end{aligned}\tag{11}$$

Since the fidelity term is also given by the covariant gradient of the squared fidelity energy, the fidelity error should be projected onto the tangent space $\mathbf{T}_{\mathbf{w}(x,y)}$. Thus, all the updating terms for the time-evolution of the chromaticity component $\mathbf{w}(x,y)$ are projected onto the tangent space $\mathbf{T}_{\mathbf{w}(x,y)}$. In addition, since the auxiliary vector functions $\mathbf{u}$, $\mathbf{v}$ live on the tangent space $\mathbf{T}_{\mathbf{w}(x,y)}$, their updated vectors should be projected onto the tangent space $\mathbf{T}_{\mathbf{w}(x,y)}$.

For the chromaticity component $\mathbf{w}$, the time-evolution equations are modified as follows:

$$\begin{aligned}\partial_\tau \mathbf{w} &= \partial_x^*\left(g(\gamma)\cdot\partial_x\mathbf{w}\right)+\partial_y^*\left(g(\gamma)\cdot\partial_y\mathbf{w}\right)-s_{\mathbf{w}}\cdot\left(\partial_x^*\mathbf{u}+\partial_y^*\mathbf{v}\right)\\ &\quad-\lambda_{\mathbf{w}}\cdot\Pi_{\mathbf{w}(x,y)}\left(\mathbf{w}-\mathbf{I}\right)\\ &=\Pi_{\mathbf{w}(x,y)}\left\{\partial_x\left(g(\gamma)\cdot\partial_x\mathbf{w}\right)+\partial_y\left(g(\gamma)\cdot\partial_y\mathbf{w}\right)\right.\\ &\quad\left.-s_{\mathbf{w}}\cdot\left(\partial_x\mathbf{u}+\partial_y\mathbf{v}\right)-\lambda_{\mathbf{w}}\cdot\left(\mathbf{w}-\mathbf{I}\right)\right\},\end{aligned}\tag{12.1}$$

$$\begin{aligned}\partial_\tau \mathbf{u} &= \partial_x^*\left(g\left(|\nabla\mathbf{u}|\right)\cdot\partial_x\mathbf{u}\right)+\partial_y^*\left(g\left(|\nabla\mathbf{u}|\right)\cdot\partial_y\mathbf{u}\right)-\lambda_{\mathbf{u}}\cdot\left(\mathbf{u}-\partial_x^*\mathbf{w}\right)\\ &=\Pi_{\mathbf{w}(x,y)}\left\{\partial_x\left(g\left(|\nabla\mathbf{u}|\right)\cdot\partial_x\mathbf{u}\right)+\partial_y\left(g\left(|\nabla\mathbf{u}|\right)\cdot\partial_y\mathbf{u}\right)\right.\\ &\quad\left.-\lambda_{\mathbf{u}}\cdot\left(\mathbf{u}-\partial_x\mathbf{w}\right)\right\},\end{aligned}\tag{12.2}$$

$$\begin{aligned}\partial_\tau \mathbf{v} &= \partial_x^*\left(g\left(|\nabla\mathbf{v}|\right)\cdot\partial_x\mathbf{v}\right)+\partial_y^*\left(g\left(|\nabla\mathbf{v}|\right)\cdot\partial_y\mathbf{v}\right)-\lambda_{\mathbf{v}}\cdot\left(\mathbf{v}-\partial_y^*\mathbf{w}\right)\\ &=\Pi_{\mathbf{w}(x,y)}\left\{\partial_x\left(g\left(|\nabla\mathbf{v}|\right)\cdot\partial_x\mathbf{v}\right)+\partial_y\left(g\left(|\nabla\mathbf{v}|\right)\cdot\partial_y\mathbf{v}\right)\right.\\ &\quad\left.-\lambda_{\mathbf{v}}\cdot\left(\mathbf{v}-\partial_y\mathbf{w}\right)\right\}.\end{aligned}\tag{12.3}$$

The actual iterative discrete algorithm is as follows:

[Iterative discrete algorithm for the chromaticity component $\mathbf{w}$]

In the following, $\mathbf{w}$ on the pixel location (i, j) at the τ iteration is denoted by $\mathbf{w}_{i,j}^{(\tau)}$.

0) Initial setting:

$$\begin{aligned}&\mathbf{w}_{i,j}^{(0)}=\mathbf{I}_{i,j}\Big/\left\|\mathbf{I}_{i,j}\right\| \quad;\quad \mathbf{u}_{i,j}^{(0)}=\Pi_{\mathbf{w}_{i,j}^{(0)}}\left\{\left(\mathbf{w}_{i+1,j}^{(0)}-\mathbf{w}_{i-1,j}^{(0)}\right)\Big/2\right\}\\ &\qquad\qquad;\quad \mathbf{v}_{i,j}^{(0)}=\Pi_{\mathbf{w}_{i,j}^{(0)}}\left\{\left(\mathbf{w}_{i,j+1}^{(0)}-\mathbf{w}_{i,j-1}^{(0)}\right)\Big/2\right\}\end{aligned}\tag{13}$$

1) Update of $\mathbf{u}$:

$$\begin{aligned}\mathbf{u}_{i,j}^{(\tau+1)}=\Pi_{\mathbf{w}_{i,j}^{(\tau)}}\Bigg[\ \mathbf{u}_{i,j}^{(\tau)}+\varepsilon\cdot\Bigg\{&\sum_{d=N,S,E,W}\left\{g\left(\left|\nabla_d\mathbf{u}_{i,j}^{(\tau)}\right|\right)\cdot\nabla_d\mathbf{u}_{i,j}^{(\tau)}\right\}\\ &-\lambda_{\mathbf{u}}\cdot\left(\mathbf{u}_{i,j}^{(\tau)}-\frac{1}{2}\cdot\left(\mathbf{w}_{i+1,j}^{(\tau)}-\mathbf{w}_{i-1,j}^{(\tau)}\right)\right)\Bigg\}\ \Bigg]\end{aligned}\tag{14}$$

2) Update of $\mathbf{v}$:

$$\begin{aligned}\mathbf{v}_{i,j}^{(\tau+1)}=\Pi_{\mathbf{w}_{i,j}^{(\tau)}}\Bigg[\ \mathbf{v}_{i,j}^{(\tau)}+\varepsilon\cdot\Bigg\{&\sum_{d=N,S,E,W}\left\{g\left(\left|\nabla_d\mathbf{v}_{i,j}^{(\tau)}\right|\right)\cdot\nabla_d\mathbf{v}_{i,j}^{(\tau)}\right\}\\ &-\lambda_{\mathbf{v}}\cdot\left(\mathbf{v}_{i,j}^{(\tau)}-\frac{1}{2}\cdot\left(\mathbf{w}_{i,j+1}^{(\tau)}-\mathbf{w}_{i,j-1}^{(\tau)}\right)\mathbf{u}_{i,j}^{(\tau)}\right)\Bigg\}\ \Bigg]\end{aligned}\tag{15}$$

3) Update of $\mathbf{w}$:

3-1) Calculation of the tentative vector $\mathbf{p}$:

$$\begin{aligned}\mathbf{p}_{i,j}=\mathbf{w}_{i,j}^{(\tau)}+\varepsilon\cdot\Pi_{\mathbf{w}_{i,j}^{(\tau)}}\Bigg[&\sum_{d=N,S,E,W}\left\{g(\gamma)\cdot\nabla_d\mathbf{w}_{i,j}^{(\tau)}\right\}-\lambda_{\mathbf{w}}\cdot\left(\mathbf{w}_{i,j}^{(\tau)}-\mathbf{I}_{i,j}\right)\\ &-\frac{s_{\mathbf{w}}}{2}\cdot\left\{\left(\mathbf{u}_{i+1,j}^{(\tau+1)}-\mathbf{u}_{i-1,j}^{(\tau+1)}\right)+\left(\mathbf{v}_{i,j+1}^{(\tau+1)}-\mathbf{v}_{i,j-1}^{(\tau+1)}\right)\right\}\Bigg]\end{aligned}\tag{16}$$

3-2) Under-clipping of the tentative vector $\mathbf{p}$:

$$\mathbf{q}_{i,j}=\Theta\left\{\mathbf{p}_{i,j}\right\}\ ;\ \left[\Theta(\mathbf{a})\right]_{(n)}=\begin{cases}\left[\mathbf{a}\right]_{(n)} & ,\ \text{if}\ \left[\mathbf{a}\right]_{(n)}\ge 0\\ 0 & ,\ \text{if}\ \left[\mathbf{a}\right]_{(n)}<0\end{cases}\tag{17}$$

3-3) Normalization of the tentative vector $\mathbf{q}$:

$$\mathbf{w}_{i,j}^{(\tau+1)}=\mathbf{q}_{i,j}\Big/\left\|\mathbf{q}_{i,j}\right\|\tag{18}$$

[End of the algorithm]

In the discrete algorithm for the chromaticity component $\mathbf{w}$, if we fix the parameter ε of the updating speed and the parameter K in the edge-stopping function g at constant values irrespectively of the brightness component r, it may incur unevenness in improvements in image sharpness and noiselessness. To cope with this problem, we control the parameters ε, K as functions of the brightness component r of the input color image $\mathbf{I}$ as follows:

$$\varepsilon_{i,j}=\varepsilon_0\cdot\left\|\mathbf{I}_{i,j}\right\|^{-1}\ ,\ \varepsilon_0:\text{small positive constant},\tag{19}$$

$$\begin{aligned}&K_{i,j}=\sigma_N\Big/\left\|\mathbf{I}_{i,j}\right\|\ ,\\ &\quad\sigma_N:\text{standard deviation of additive Gaussuan noise}\\ &\qquad\text{in an input noisy blurred image}.\end{aligned}\tag{20}$$

5. PERFORMANCE EVALUATIONS

5.1 Test color images and performance measures

We evaluate performance of our schemes using artificially blurred test color images. First we blur an original sharp color image $\mathbf{P}(x,y)$, given in primary color components,

$$\mathbf{P}(x,y)=\left(\ P_R(x,y),\ P_G(x,y),\ P_B(x,y)\ \right)^T,\tag{21}$$

with the circular blurring filter having the impulse response h,

$$h(x,y;r)=\begin{cases}\dfrac{1}{2\pi r^2} & ,\ if\ \left(x^2+y^2\right)\le r\\ 0 & ,\ if\ \left(x^2+y^2\right)>r\end{cases},\tag{22}$$

and then add random Gaussian noise to the blurred color image h*$\mathbf{P}(x, y)$; thus we generate an artificially blurred test color image $\mathbf{Q}(x, y)$, given in primary color components. Let $\mathbf{R}(x, y)$ denote the sharpness-enhanced color image reproduced from the blurred test color image $\mathbf{Q}(x, y)$.

For the performance evaluation, we define the quantitative measures [8] in the primary color space as follows.

1) Peak SNR of the sharpened color image $\mathbf{R}$: PSNR [dB] is computed between the original sharp color image $\mathbf{P}$ and the sharpened color image $\mathbf{R}$.

2) Blur-Removal Ratio Br and Noise-Removal Ratio Nr : Let the vectors, $\mathbf{b}$, $\mathbf{n}$, $\mathbf{s}$, denote circular image blurs artificially added to the original color image $\mathbf{P}$, random Gaussian noise added to the circularly blurred color image h*$\mathbf{P}$, and deviations of the artificially blurred test color image $\mathbf{Q}$ from the sharpened color image $\mathbf{R}$, i.e. $\mathbf{Q} - \mathbf{R}$, respectively. We define those vectors, $\mathbf{b}$, $\mathbf{n}$, $\mathbf{s}$, by arranging their values of the three primary colors at all the pixels in one column. Then, we define Br and Nr as follows:

$$\mathrm{Br}=\left(\mathbf{b},\mathbf{s}\right)\Big/\left\|\mathbf{b}\right\|^2\quad,\quad\mathrm{Nr}=\left(\mathbf{n},\mathbf{s}\right)\Big/\left\|\mathbf{n}\right\|^2\ .\tag{23}$$

The positive value of Br / Nr means that the blur / noise removal is successfully achieved. If blur / noise is perfectly removed, then the value of Br / Nr will be 1; but the reverse is not necessarily true. On the contrary, the negative value means that the blur / noise is augmented far from being removed.

3) Artifact-Component Ratio Ar : We define Ar as follows:

$$\begin{aligned}&\mathrm{Ar}=\left\|\left(\mathbf{I}-\mathbf{A}\cdot\left(\mathbf{A}^T\cdot\mathbf{A}\right)^{-1}\cdot\mathbf{A}^T\right)\cdot\mathbf{s}\right\|\Big/\left\|\mathbf{s}\right\|\ ,\\ &\qquad\mathbf{A}=\left[\ \mathbf{b}\ ,\ \mathbf{n}\ \right]\ ,\ \mathbf{I}:\text{identity matrix}.\end{aligned}\tag{24}$$

Ar is given by the ratio of the norm of the projection of $\mathbf{s}$ onto the orthogonal complement of the linear subspace spanned by $\mathbf{b}$ and $\mathbf{n}$, to the norm of $\mathbf{s}$, and it quantifies how far the enhancement signal component -$\mathbf{s}$, produced by the sharpening algorithm, contains undesirable artifacts irrelevant to the compensation for $\mathbf{b}$ and $\mathbf{n}$. If no artifact occurs, then the value of Ar will be 0.

5.2 Evaluation results

Fig.1 shows the original color images used for the performance evaluations. Table 1 shows the values of PSNR, Br, Nr and Ar for the color images sharpened by our new CB-scheme and our previous V-scheme. As shown in Table 1, for the images other than the monochrome stripe image, our new CB-scheme gives a higher PSNR than the V-scheme, and with regard to the other quantitative measures, Br, Nr, Ar, our new CB-scheme outperforms our previous V-scheme. For monochrome images, the chromaticity-brightness model does not work so well. Fig.2 and Fig.3 compare the same portions of color images sharpened by our new CB-scheme with those sharpened by our previous V-scheme. Though the V-scheme sharpens blurred step edges to steeper edges, it does not necessarily enhance contrasts of blurred intensity variations in very complex texture image regions so well as in simple step-edge regions. On the other hand, our new CR-scheme sharpens not only blurred step edges but also blurred complex textures to some extent. Our CR-scheme achieves the selective color-image sharpening with a subjectively superior quality.

6. CONCLUSIONS

The quantitative evaluations using artificially blurred test images demonstrate that our new CR-scheme sharpens blurred color edges and complex textures selectively better than our previous V-scheme. We are studying the application of our schemes to the real image processing problems: pre-processing and post-processing for demosaicking, motion de-blurring, suppression of breathing distortions, and so on.

REFERENCES

[1] A. Rosenfeld and A.C. Kak, *Digital Picture Processing*, Ch.6.4.2., Academic Press, Inc., New York, USA, 1982.

[2] G. Aubert and P. Kornprobst, *Mathematical Problems in Image Processing – Partial Differential Equations and The Calculus of Variations*, Springer Verlag, New York, USA, 2002.

[3] G. Auber and L. Vese, *A Variational Method in Image Recovery*, SIAM J. Num. Anal., **34**, 5, pp.1948-1979, 1997

[4] P. Perona and J. Malik, *Scale-Space and Edge Detection Using Anisotropic Diffusion*, IEEE Trans. Pattern. Anal. & Mach. Intell., **12**, 7, pp.629-639, 1990.

[5] S. Osher and L.I. Rudin, *Feature-Oriented Image Enhancement Using Shock Filters*, SIAM J. Num. Anal., **27**, 4, pp.919-940, 1990.

[6] M. Proesmans, E.J. Pauwels and L.J. Van Gool, *Coupled Geometry Driven Diffusion Equations for Low-Level Vision*, pp.191-228, in Geometry-Driven Diffusion in Computer Vision, B.M. ter Haar Romeny Ed., Kluwer Academic Publishers, Dordrecht, The Netherlands, 1994.

[7] G. Gilboa, N. Sochen and Y. Zeevi, *Forward-and-Backward Diffusion Processes for Adaptive Image Enhancement and Denoising*, IEEE Trans. Pattern. Image Process., **11**, 7, pp.680-703, 2002.

[8] T. Saito, J. Satsumabayashi, K. Yashiro and T. Komatsu, *Selective Image Sharpness Enhancement by Coupled Nonlinear Reaction-Diffusion Time-Evolution and Its Practical Application*, Proc. EUSIPCO 2002, pp.II445-II448, Toulouse, France, 2002.

[9] T. Saito, H. Harada, J. Satsumabayashi and T. Komatsu, *Color Image Sharpening Based on Nonlinear Reaction-Diffusion*, Proc. IEEE ICIP, pp.III389-III392, Barcelona, Spain, 2003.

[10] T. Saito, H. Harada, J. Satsumabayashi and T. Komatsu, *Selective Sharpening of Color Images Through Coupled Nonlinear Diffusion Process*, J. Institute of Image Information & Television Engineers, **58**, 11, pp.1673-1679, 2004.

[11] T. Saito, H. Harada, and T. Komatsu, *Extension of Coupled Nonlinear Diffusion to Motion De-blurring*: *Introduction of Anisotripic Peaking*, J. Institute of Image Information & Television Engineers, **58**, 12, pp.1839-1844, 2004.

[12] F. Catte, P. L. Lions, J.M. Morel and T. Coll, *Image Selective Smoothing and Edge Detection by Nonlinear Diffusion*, SIAM J. Num. Anal., **29**., 1, pp.182-193, 1992.

[13] P.E. Trahanias and A.N. Venetsanpoulos, *Vector Directional Filters - A New Class of Multichannel Image Processing Filters*, IEEE Trans. Image Process., **2**, 4, pp.528-534, 1993.

[14] P.E. Trahanias, D. Karako and A.N. Venetsanpoulos, *Directional Processing of Color Images* : *Theory and Experimental Results*, IEEE Trans. Image Process., **5**, 6, pp.868-880, 1996.

[15] K.N. Plataniotis, B. Smolka and K. Martin, *Vector Filtering for Color Imaging*, IEEE Signal Processing Magazine, **22**, 1, pp.74-86, 2005.

[16] B. Tang, G. Sapiro and V. Caselles, *Diffusion of General Data on Non-Flat Manifolds via a Harmonic Map Theory*, International Journal of Computer Vision, **36**, 2, pp.149-161, 2000.

[17] T.F. Chen and J. Shen, *Variational Restoration of Non-Flat Image Features* : *Model and Algorithms*, CAM Technical report, 99-20, UCLA, 1999.

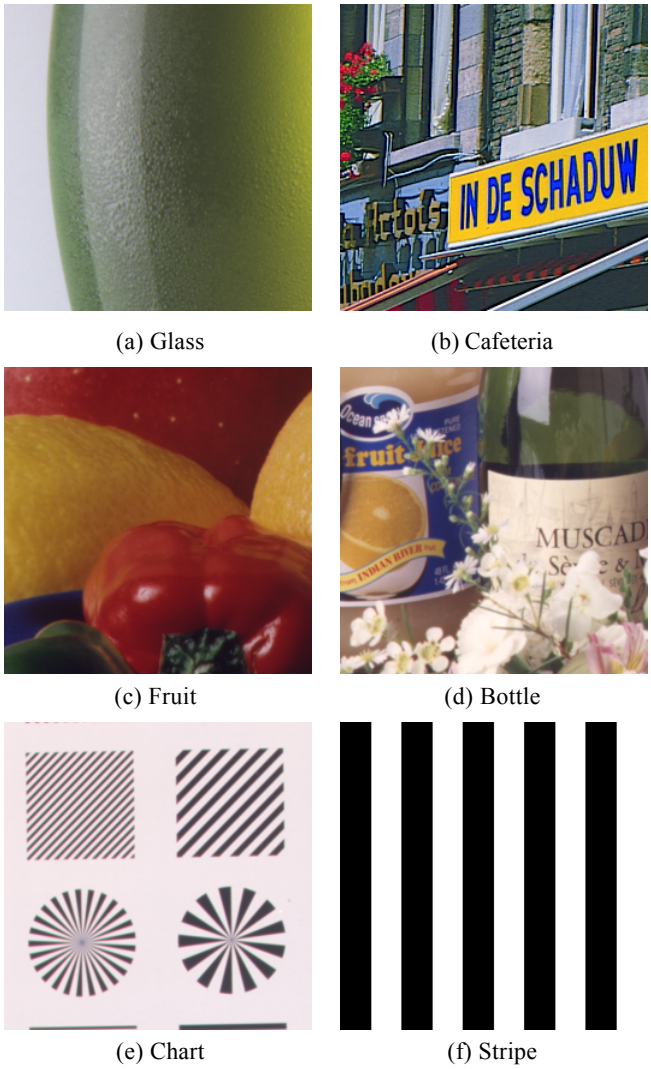

(a) Glass (b) Cafeteria

(c) Fruit (d) Bottle

(e) Chart (f) Stripe

Figure 1 - Original sharp color images used for the simulations

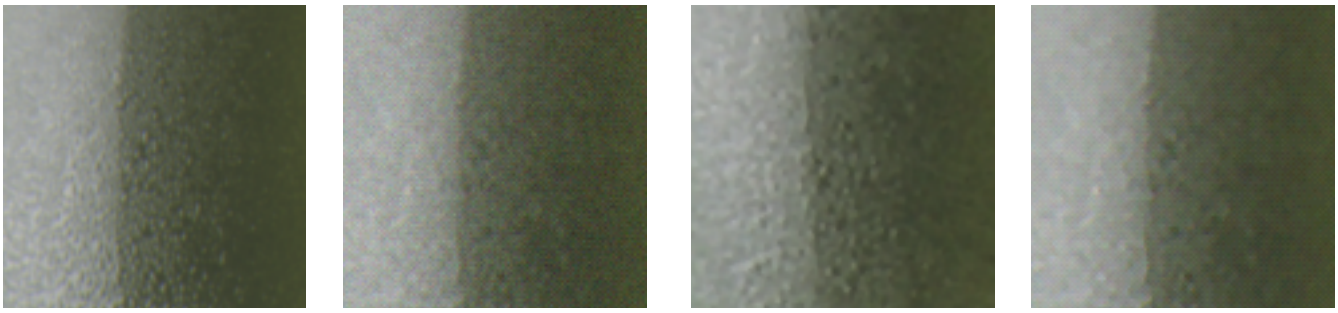

(a) Original sharp image

(b) Blurred test image (PSNR = 33.086 dB)

(c) Sharpened image by our new CB-scheme (PSNR = 36.894 dB)

(d) Sharpened image by our previous V-scheme (PSNR = 36.492 dB)

Figure 2 - Original sharp image, blurred test image and sharpened images

(a) Original sharp image

(b) Blurred test image (PSNR = 22.101 dB)

(c) Sharpened image by our new CB-scheme (PSNR = 24.450 dB)

(d) Sharpened image by our previous V-scheme (PSNR = 24.078 dB)

Figure 3 - Original sharp image, blurred test image and sharpened images

Table 1 - Selective sharpening performance of our new CB-scheme and our previous V-scheme for the blurred test images

Blurred image	Methods	PSNR [dB]	Br	Nr	Ar
Glass	CB-Scheme	**36.894**	-0.071	0.736	0.476
33.086 [dB]	V-Scheme	36.492	-0.185	0.686	0.43
Cafeteria	CB-Scheme	**24.45**	0.441	0.092	0.753
22.101 [dB]	V-Scheme	24.078	0.403	-0.149	0.767
Fruit	CB-Scheme	**40.011**	-0.1	0.78	0.358
33.695 [dB]	V-Scheme	39.994	0.14	0.756	0.424
Bottle	CB-Scheme	**34.799**	0.394	0.661	0.635
31.236 [dB]	V-Scheme	34.256	0.456	0.534	0.704
Chart	CB-Scheme	**33.329**	0.752	0.548	0.547
28.254 [dB]	V-Scheme	33.068	0.745	0.509	0.56
Stripe	CB-Scheme	38.753	0.877	0.837	0.183
25.091 [dB]	V-Scheme	**39.636**	0.902	0.811	0.164